

Elsevier

Scientific African

Volume 19, March 2023, e01489

Scientific African

Application of ginger and grapefruit essential oil extracts on the corrosion inhibition of mild steel in dilute 0.5 M H₂SO₄ electrolyte

Author links open overlay panel

Roland Tolulope Loto a

,

Moses M. Solomon b

a

Department of Mechanical Engineering, Covenant University, Ota, Ogun State, Nigeria

b

Department of Chemistry, Covenant University, Ota, Ogun State, Nigeria

Received 18 June 2022, Revised 14 November 2022, Accepted 6 December 2022, Available online 9 December 2022, Version of Record 20 December 2022.

What do these dates mean?

Cite

<https://doi.org/10.1016/j.sciaf.2022.e01489>

Get rights and content

Under a Creative Commons license

open access

Abstract

Admixture of ginger and grapefruit essential oils (GPP) were studied for their corrosion inhibition properties on mild steel (MS) in 0.5 M H₂SO₄ solution by potentiodynamic polarization, open circuit

potential measurement, electrochemical impedance spectroscopy, weight loss analysis and ATF-FTIR spectroscopy. Results from potentiodynamic polarization shows GPP significantly reduced the corrosion of MS from 8.430 mm/y at 0% GPP concentration to values between 1.979 mm/y and 0.565 mm/y. The corresponding inhibition efficiency values ranged from 76.52% to 93.5% and corrosion current density from 1.88×10^{-4} A/cm² to 5.36×10^{-5} A/cm². GPP displayed mixed-type inhibition at all GPP concentrations studied. The OCP plot at 0% GPP initiated at -0.495V compared to -0.443V and -0.451V at 1% and 3.5% GPP. At 9000s, the corresponding OCP values are -0.442V, -0.410V and -0.424V due to electropositive plot shift and passivation of MS surface at 1% and 3.5% GPP, though significant potential transients were present on the OCP plot at 1% GPP. The electrochemical impedance results indicate that the corrosion resistance of MS increased from 4.402 Ω cm² to 99.318 Ω cm² upon the addition of 3.5% GPP resulting in inhibition efficiency of 96%. Data from weight loss analysis shows decrease in corrosion rate from 184.48 mm/y to values between 8.94 mm/y and 6.25 mm/y. The corresponding inhibition efficiency values varies from 95.16% at 1% GPP to 96.61% at 3.5% GPP concentration. The ATF-FTIR results confirm the adsorption of GPP molecules on the surface of the carbon steel electrode.

Previous article in issue

Next article in issue

Keywords

Carbon steelCorrosion managementEssential oilInhibitionEnvironmental degradation

Introduction

The economic value of carbon steels in addition to their versatile mechanical and physical properties accounts for their universal utilization in industrial and domestic environments worldwide [16]. They can be quenched, tempered, fabricated, welded and easily formed to desired specifications. Carbon steels combine strength with excellent ductility, hardenability and carburization properties. Utilization of carbon steels covers their usage as cold headed fasteners and bolts, shafts, sprockets, spindles, pins, crankshafts, couplings, rods and other high volume component devices. Carbon steel makeup 85% of the total steel production globally [34]. However, the steel is prone to significant damage resulting from corrosion [11], [17], [39]. The corrosion problem is due to the application of the steel in petrochemical, gas processing, automobile, construction, fertilizer production, desalination and extraction industries containing sulphates a major component of H₂SO₄ acid. This stems from the weak resistance of the steel to the electrochemical action of sulphates on the steel surface as a result of their inability to passivate within such environments. The oxide formed on the steel exhibits numerous pores enabling the electrolytic transport and diffusion of the corrosive species onto the substrate Fe. Passivating elements (Cr, Ni, Mo etc.) are responsible for the evolution of an impenetrable film and passivation on stainless steels [41]. H₂SO₄ acid is a universal commodity solution whose synthesis and production is an important reference point for a nation's industrial capacity. The solution is produced through a variety of techniques e.g. wet H₂SO₄ process, contact process etc. The acid is used in the production of fertilizers, petrochemical refining and production, chemical processing, production of dyes, batteries and bleaching agent, removal of metals from their ores and in rubber production [26], [48], [53]. The consequence of carbon steel corrosion in H₂SO₄ is high economic damage, decrease in operational lifespan, plant shutdowns, industrial accidents and enormous cost of repair and maintenance [1], [4], [63]. Corrosion prevention on carbon steels can be substantially reduced with customized corrosion

control techniques that factors in the peculiarities of application and environmental conditions. Techniques such as surface modification, electrodeposition, electroplating, cathodic protection, paint coatings etc. have been proven to be effective but are limited in application and are costly. Fluid compounds identified as corrosion inhibitors have been proven to be effective, economical and versatile in corrosion prevention of carbon steels [47]. Although, corrosion inhibitors (i.e. inorganic and organic inhibitors) have been known for decades the confirmed effective ones have been shown to be toxic to the environment and personnel leading to restriction on their use by government regulations [12], [36], [40], [42], [57], [66]. Green chemical compounds from plant extracts have shown promising corrosion inhibition characteristics. However, they tend to perform poorly, they are biodegradable, have short shelf life and lack strong adsorption performance on carbon steels [5], [14], [43], [45], [56]. Other results obtained from experimental investigations on green chemical compounds depict the importance of well documented repository inhibition effect, reactive species, effective functional lifespan and adsorptive properties [3], [38], [44], [51], [55]. Distillates from essential oils (plants, barks, seeds etc.) has been research into [8], [10], [18], [19], [24], [30], [37], [45]. Results obtained by Znini [68], Bathily et al [69] and Hossain et al [31] from over two hundred published manuscripts on the corrosion performance of various essential oils extracts. showed that they performed effectively especially when related to their concentration and chemical properties. Nevertheless, the absence and toxic compounds in their natural forms, their abundance, renewability and environmental sustainability gives room for extensive research for corrosion inhibition. This also brings up the problem of documentation. One of the features of this article in addition to the problems earlier raised is to determine the threshold concentration for optimal performance of plant extracts. It's must be noted that essential oil distillates have been proven to be marginally effective but their corrosion inhibition effect highly dependent on concentration [13], [15], [46], [60], [61]. Fidrulli et al [22] studied the effect of ginger extracts and powder on the corrosion inhibition of mild steel in 1M HCl solution. Results showed inhibition efficiency increased with respect to ginger concentration with optimal inhibition efficiency of 91% and 86% from weight loss and polarization test. Narenkumar et al [50] studied the effect of ginger extract on the microbial (*Bacillus thuringiensis* EN2) corrosion resistance of mild steel in a cooling water system. The extract was observed to form a protective layer to prevent the biofilm formation. Maximum inhibition efficiency of 80% was obtained. Fouda et al [23] studied the effect of ginger extract on steel corrosion in sulfide polluted NaCl solution. Inhibition efficiency was observed to increase with inhibitor concentration with optimal value of 83.9% at 250 ppm of ginger. Gadaw and Motawea [25] Studied the inhibitive effect of ginger roots extract on carbon steel corrosion in 1.0 M HCl solution at specific temperatures. Results showed inhibition efficiency increased with increase in concentration of the extract and decrease in temperature. Maximum inhibition efficiency of 94% at 200 ppm of extract and 25°C was attained. Batah et al [6] studied grapefruit oil extract as corrosion inhibitor on carbon steel in 1M HCl. Inhibiting action increased with extract concentration with highest efficiency of 86.15% at 1g/L of the extract. In support of the quest for effective green corrosion inhibitors for carbon steels, this research focusses on the protection effect of equal admixture ginger and grapefruit on mild steel in 0.5M H₂SO₄ solution. The purpose of the admixture is to study the synergistic effect of the two extracts and observed for significant variation in corrosion inhibition compared to their separate performances.

Experimental methods

Materials and preparation

Mild steel (MS) test sample with circular configuration of 1.2 cm diameter has elemental composition of 0.21% Cu, 0.29% Si, 1.04% Mn, 0.27% C, 0.06% S, 0.05% P and 98.08% Fe from energy dispersive spectroscopy analysis with PhenomWorld scanning electron microscope. The MS sample was divided into several smaller test samples with manual cutting tool into average dimensions of 1 cm length for weight loss measurement. MS test pieces for potentiodynamic polarization and open circuit potential analysis were attached to a Cu cable with lead before implanting in pre-hardened acrylic mixture. The visible surface of the steel was abraded with emery papers (60, 300, 600, 1000 and 1500 grits) and polished with 6 μm diamond fluid before washing with distilled H₂O and propanone. Ginger and grapefruit (GPP) essential oil extracts were purchased from NOW Foods, USA, and prepared in volumetric concentrates of 0%, 1%, 1.5%, 2%, 2.5%, 3% and 3.5% respectively per 200ml of 0.5M H₂SO₄ solutions at ratio 1:1.

Potentiodynamic polarization and open circuit potential measurement

Electrochemical analysis was carried out at 35 °C room temperature with a Digi-Ivy 2311 potentiostat (consisting of triple electrode configuration within a transparent beaker containing the acid-extract solution) and connected to a computer. The electrodes are MS electrodes with exposed surface area of 1.13 cm², Ag/AgCl standard electrode and Pt wire auxiliary electrode. Polarization plots were produced at scan rate of 0.0015 V/s from -1.1 V and +1.65 V. Corrosion current density C_j (A/cm²) and corrosion potential, C_p (V) values were determined through Tafel derivation. Corrosion rate, CRT (mm/y) was computed from the mathematical relationship below;

(1)

where C_q is the correlative weight (g) of MS, 0.00327 is the corrosion constant and D is density (g/cm³). Inhibition efficiency, IEF (%) was calculated from below;

(2)

CRT1 and CRT2 are MS weight loss without and with the extracts. Polarization resistance, P_R (Ω) was computed from below;

(3)

B_a and B_c are the anodic and cathodic Tafel slopes (V/dec). Open circuit potential measurements were performed at step potential of 0.2V/s for 9000 s in 0.5 M H₂SO₄ solution at 0%, 1% and 3.5% GPP concentration with the same electrode configuration as the potentiodynamic polarization test.

Electrochemical impedance spectroscopy

A Gamry Potentiostat/Galvanostat/ZRA Reference 600 + workstation was used for the electrochemical impedance spectroscopy (EIS) experiments. The experiments were carried utilizing the high carbon steel sample as the working electrode, a Ag/AgCl (sat. 4.2 M KCl) as the electrode, and a platinum rod as the counter electrode. Before the impedance characteristics of the working electrode were obtained, the open circuit potential was monitored for 1800 s. At the open circuit potential, the EIS measurements were performed under potentiostatic mode by applying an alternating-current signal with amplitude of 10 mV over a frequency range of 100,000 Hz to 0.1 Hz. The electrochemical impedance data obtained were analysed using the Echem analyst software.

Weight loss measurement

Weight of MS steel test pieces were determined and singularly suspended in 200 mL of the acid-extract solution for 240 h. MS weight determination was done at 24 h interval. Corrosion rate, CRT (mm/y) was determined from the relationship below;

(4)

WL is the weight loss (g), D is the density (g/cm³), t represents time (h), A is the total exterior area of the MS specimen (cm²) and 87.6 is the corrosion rate constant [35]. Inhibition efficiency (η) was determined from the following numerical expression below;

(5)

WL1 and WL2 represents weight loss at specific extract concentrations.

ATF-FTIR spectroscopy

1% GPP concentration/0.5 M H₂SO₄ solution, before and following corrosion test were analysed under infrared particle emissions with Bruker Alpha FTIR (Fourier transform infrared spectroscopy) spectrometer within the wavelength span of 375 to 7500 cm⁻¹, and accuracy of 0.9 cm⁻¹ after 240 h of MS weight loss measurement. Spectral patterns were studied and linked to the conventional ATF-FTIR (Attenuated Total Reflectance-Fourier transform infrared spectroscopy) table. Tabulations were done for the reactive groups which influenced the redox reaction processes.

Results and discussion

Potentiodynamic polarization studies

Cathodic and anodic polarization plots representing the corrosion polarization behavior of MS in 0.5 M H₂SO₄ solution at 1% - 3.5% GPP concentration are shown in Fig. 1. The polarization data retrieved from the plots are shown in Table 1. Observation of Table 1 shows MS corrosion rate value at 0% GPP concentration significantly varies from the corrosion rate at 1%-3.5% GPP concentration in relative manner compared to the observation from weight loss analysis. Corrosion rate at 0% GPP concentration is 8.430 mm/y corresponding to corrosion current density value of 8×10^{-4} A/cm² and polarization resistance of 28.42 Ω . The corresponding polarization plot configuration shows significantly higher cathodic slope was observed compared to the anodic polarization slope which intersects at -0.449 V. The relatively higher cathodic and anodic polarization slope is due to accelerated cathodic reactions involving O₂ reduction and H₂ evolution, and anodic reactions involving surface oxidation of the steel [64]. However, beyond 0% GPP concentration significant decrease in the cathodic polarization slope was observed due to suppression of the cathodic half-cell reaction of the redox electrochemical process. In effect the cathodic processes were significantly slowed down with respect to GPP concentration. The anodic portion of the polarization varied marginally with respect to GPP concentration compared to the cathodic plots. This shows the anodic reactions are under activation control whereby increase in GPP concentration has limited influence on the anodic polarization behavior and inhibition of the steel. This is due to effective surface coverage of the steel irrespective of GPP concentration which will be further discussed in the weight loss measurement and optical microscopy section [47]. Addition of GPP extract to the acid solution shifts the corrosion potential of the polarization plot at all GPP concentrations positively relative to the corrosion potential at 0% GPP concentration. This signifies dominant anodic

half-cell reaction within the overall redox reaction process [7]. However, the anodic shift is less than 85mV hence GPP inhibition mechanism is mixed-type [20]. Corrosion rate of MS significantly decreased in the presence of GPP extract from 8.430 mm/y at 0% GPP concentration to 1.979 mm/y at 1% GPP concentration and values ranging between 0.719 mm/y and 0.565 mm/y (1.5% -3.5% GPP concentration). Increased in GPP concentration marginally influenced the corrosion rate of MS after 1.5% GPP concentration. At 3.5% GPP concentration, optimal inhibition efficiency was attained at 93.3%, corresponding to corrosion current density of 5.36×10^{-5} A/cm² and polarization resistance of 410.90 Ω .

Fig 1

Download: [Download high-res image \(214KB\)](#)

Download: [Download full-size image](#)

Fig. 1. Potentiodynamic polarization plots for MS corrosion in 0.5M H₂SO₄ solution at 0%-3.5% GPP concentration

Table 1. Potentiodynamic polarization data for MS corrosion in 0.5M H₂SO₄ solution at 0%-3.5% GPP concentration

GPP Concentration (%)	MS CRT (mm/y)	GPP IEF (%)	Corrosion Current (A)	CJ (A/cm ²)	CP (V)
PR (Ω)	Bc (V/dec)	Ba (V/dec)			
0	8.430	-	9.04E-04	8.00E-04	-0.449 28.42 -9.662 6.331
1	1.979	76.52	2.12E-04	1.88E-04	-0.409 121.10 -4.670 0.920
1.5	0.719	91.47	7.71E-05	6.83E-05	-0.435 303.10 -6.135 0.840
2	0.592	92.98	6.35E-05	5.62E-05	-0.433 331.30 -3.422 0.640
2.5	0.588	93.03	6.30E-05	5.58E-05	-0.421 367.60 -2.388 0.436
3	0.579	93.13	6.21E-05	5.49E-05	-0.433 373.60 -4.309 0.286
3.5	0.565	93.30	6.05E-05	5.36E-05	-0.435 410.90 -2.816 0.812

Open circuit potential analysis

Open circuit potential (OCP) plots were produced for MS in 0.5 M H₂SO₄ solution at 0%, 1% and 3.5% GPP concentration for 9000s. The plots shown in Fig. 2 depict the active-passive transition behavior and thermodynamic properties of the surface characteristics of the steel at the metal-solution interface. The higher the corrosion rate of the steel i.e. redox electrochemical processes occurring on the steel surface. Hence, the more electronegative the plots relative to other plots [54]. The OCP plot at 0% GPP initiated at -0.495V compared to -0.443V and -0.451V for MS at 1% and 3.5% GPP concentration. The OCP plot sharply increased to electropositive values before attaining relative stability at 2019.82s (-0.453V). Beyond this point, the extent of variation of the thermodynamic properties of the steel becomes

marginal till 9000s (-0.442V). The plot configuration shows that at initiation point the steel is exposed to the electrochemical action of the corrosive species i.e. the surface is in the active phase. Between 0s and 2019.82s, there is significant transition to passive phase and stable thermodynamic behavior. This is different from passivation in Cr based alloys. In carbon steels it simply refers to the point or region at which electrochemical deterioration of the steel attains equilibrium behavior even though corrosion still occurs throughout the exposure period. Addition of GPP extract at 1% and 3.5% GPP concentration shifted MS OCP plots to electropositive values signifying decreased redox reaction processes on the steel surface [59]. This is due to passivation of the steel through surface coverage by GPP extract as presented by optical microscopy analysis. The plots initiated at -0.443V and -0.451V (as earlier stated); however, the plot at 3.5% GPP concentration attained relative thermodynamic stability at 1600s (-0.434V) and culminated at -0.424V (9000s), though marginal shift to electropositive values was observed. The OCP plot at 1% GPP concentration remained thermodynamically unstable throughout the exposure hours with visible potential transient. It must be noted that the OCP plot at 1% GPP concentration is relatively more electropositive than the plot at 3.5% GPP concentration signifying decrease in corrosion reaction processes on the steel surface. However, despite effective protection of the steel surface, the surface properties of the steel are thermodynamically unstable resulting in the potential transients. This is due to instantaneous short-term breakage of the extract protective film. The plot at 3.5% GPP concentration is more thermodynamically stable despite having a lower degree of passivation of the steel surface. This observation is due to the presence of more protonated GPP molecules available for inhibition of the corrosive species in the acid and prevention of their electrolytic transport to the steel surface. Secondly, the presence of more aggregate extract molecules possibly results in lateral among the excess extract molecules.

Fig 2

Download: [Download high-res image \(159KB\)](#)

Download: [Download full-size image](#)

Fig. 2. OCP plots for MS in 0.5 M H₂SO₄ solution at 0%, 1% and 3.5% GPP concentration

Electrochemical impedance spectroscopy studies

The electrochemical impedance characteristic of MS in 0.5M H₂SO₄ solution, without and with selected concentrations of GPP at room temperature is given in Fig. 3 in the form of (a) Nyquist and (b) Bode representations. In both the uninhibited and inhibited systems, the Nyquist diagrams exhibit a capacitive loop at the high to medium frequencies depicting the charged controlled corrosion process [21], [28], [33], [65] and an inductive loop at the low frequencies which is associated with the relaxation of the corrosion products and/or adsorbed GPP molecules [52]. These two phenomena are also evident in the Bode graphs, for instance, the broadness of the Bode Phase in Fig. 3(b). Although the MS corroded in both the uninhibited and inhibited H₂SO₄ solutions, the influence of GPP on the corrosion process is very clear. In Fig. 3(a), the introduction of 1% GPP into the corrosive solution resulted in a noticeable increase in the diameter of the capacitive loop, meaning that the presence of GPP in the corrodent delayed the charge transfer process resulting in a decrease in the rate of corrosion of the metal [21], [28], [33], [65]. The diameter of the capacitive loop (Fig. 3(a)) further increased, the Bode impedance

modulus and Phase angle shifted toward nobler values as the concentration of GPP was raised to 3.5%. This implies that the corrosion inhibition performance of GPP is concentration dependent. A further inspection of the Nyquist graphs reveals that the capacitive loop is not a perfect circle which is a common feature of a solid electrode and describes the frequency dispersion caused by the heterogeneity of the working MS electrode [67]. The nature of the impedance spectra (Fig. 3) prompted the selection of the two-time constants equivalent circuit given in Fig. 4 to model the impedance data. The suitability of the selected equivalent circuit is reflected in the low fitting error and Chi square values given in Table 2. The elements of the equivalent circuit have the following meaning: R_s = solution resistance), R_{ct} = charge transfer resistance, \varnothing = constant phase element, R_f = film resistance, and R_L and L are the inductive elements. The use of \varnothing instead of a capacitor was necessitated by the imperfectness nature of the impedance [Fig. 3(a)] [32]. The impedance of \varnothing can be defined as [33]:

(6)

where

is the \varnothing constant, n is the CPE exponent and describes the heterogeneity of the electrode, j is an imaginary number, and w the angular frequency in rad/s. The fitted values and the inhibition efficiency calculated using Equation 2 are given in Table 2.

(7)

Fig 3

Download: [Download high-res image \(314KB\)](#)

Download: [Download full-size image](#)

Fig. 3. Electrochemical impedance plots for MS corrosion in 0.5M H₂SO₄ solution without and with selected concentrations of GPP at room temperature in (a) Nyquist and (b) Bode representations.

Fig 4

Download: [Download high-res image \(73KB\)](#)

Download: [Download full-size image](#)

Fig. 4. Equivalent circuit used in the analysis of the electrochemical impedance data obtained for the corrosion of MS corrosion in 0.5M H₂SO₄ solution without and with selected concentrations of GPP at room temperature.

Table 2. Electrochemical impedance parameters for MS in 0.5M H₂SO₄ solution without and with selected concentrations of GPP at 30°C

Empty Cell	Empty Cell	CPEd \pm Er	Empty Cell	Empty Cell
------------	------------	---------------	------------	------------

Conc. (%)	Rs ± Er (Ω cm ²)	Y01 (μΩ-1 s ² cm ⁻²)	n1	Rct± Er (Ω cm ²)	IE (%)
0	0.103±0.002	272.20±0.00	0.97±0.71	3.961±0.11	-
1	1.014±0.024	194.05±0.00	0.93±0.29	26.000±7.08	85
3.5	0.642±0.008	132.30±0.00	0.88±0.00	98.930±14.75	96
CPEf± Er					
Y02 (μΩ-1 s ² cm ⁻²)	n2	Rf± Er (Ω cm ²)	Rtotal (Ω cm ²)	L (Ω s cm ²)	
(× 10 ⁻³)					
127.90±0.00	0.99±0.05	0.441±0.112	4.402	3.97E-9	84.40
92.50±0.00	0.93±0.16	3.357±7.097	29.357	8.32E-4	5.60
82.00±0.00	0.63±0.11	0.388±0.007	99.318	4.86E-4	0.98

In Table 2, both the Y01 and Y02 are seen to decrease with increase in the concentration of GPP. This is reflective of the improvement in the characteristics of the adsorbed steel surface film. Generally, Y0 gives information about the characteristics of a metal surface film [62] and the smaller the Y0 value, the better the surface film [27]. It does infer that the film formed due to GPP adsorption exhibited better protective properties than the corrosion product layer. This is also evident in the high value of the total charge resistance (Rtotal) obtained for the inhibited steel surface relative to the uninhibited (Table 2). By comparing the Y0 and the Rtotal values of the 1% and 3.5% GPP systems, it is seen that, an increase in the concentration of the GPP resulted in a further decrease in the Y0 value and an increase in the Rtotal value. Consequently, the 3.5% GPP exhibited inhibition efficiency of 96% relative to 85% exhibited by 1% GPP. The decrease in the Y0 value and an increase in the Rtotal value are caused by the increase in the thickness of the electrical double layer due to adsorption of the GPP molecules onto the steel surface [2]. It is also important to mention that the n1 and n2 values are very close to unity (Table 2). This shows that the MS/H2SO4 solution interface behaved as a capacitor [27].

Weight loss analysis and optical microscopy

Weight loss analysis of MS was done for 240 h at specific concentrations of GPP extract in 0.5 M H2SO4 solution. Data obtained from the analysis (weight loss, corrosion rate and inhibition efficiency) at 240 h of exposure are presented in Table 3. Fig. 5(a) and (b) shows the plots of corrosion rate of MS and inhibition efficiency of GPP versus exposure time from 24 h to 240 h. Optical images of MS before corrosion, after corrosion without GPP extract and after corrosion with GPP extract are shown in Fig 6. The plots in Fig. 5(a) shows the significant variation of MS corrosion rate at 0% GPP concentration and MS at 1%-3.5% GPP concentration. At 0% GPP concentration, MS being a ferrous alloy without passivating elements undergoes accelerated corrosion by single displacement due to the electrochemical action of SO4²⁻ anions in the electrolyte according to the equation below;

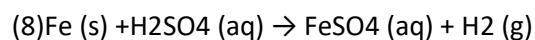


Table 3. Weight loss data for MS corrosion and GPP inhibition in 0.5 M H2SO4 solution at 240 h

GPP Extract Concentration (%)	Weight Loss (g)	Corrosion Rate (mm/y)	Inhibition Efficiency (%)
0	6.110	184.48	-
1	0.296	8.94	95.16
1.5	0.170	5.13	97.22
2	0.114	3.45	98.13
2.5	0.183	5.53	97.00
3	0.177	5.34	97.11
3.5	0.207	6.25	96.61

Fig 5

Download: [Download high-res image \(346KB\)](#)

Download: [Download full-size image](#)

Fig. 5. (a) MS corrosion rate versus exposure time at 0%-3.5% GPP concentration and (b) GPP inhibition efficiency versus exposure time at 1%-3.5% GPP

Fig 6

Download: [Download high-res image \(547KB\)](#)

Download: [Download full-size image](#)

Fig. 6. Optical images of MS

Fe oxidize in the electrolyte by losing electrons and passing into the solution as Fe^{2+} to form $FeSO_4$. H_2 gas is released through evolution mechanism resulting from the combination of H molecules. Between 24 h and 96 h, corrosion of MS increased progressively from 78.2 mm/y to 188.85 mm/y signifying increased reaction mechanism in the electrolyte. Beyond 96 h of exposure, corrosion rate of MS attained quasi stationary state before culminating at 184.48 mm/y (240 h). The image of MS (Fig. 6) at 240 h without GPP extracts showed a corroded morphology. Corrosion rate plots of MS at 1%-3.5% GPP concentration significantly decreased compared to the plot at 0% GPP concentration. This is due to inhibition effect of protonated GPP molecules which effectively suppressed the corrosion reaction processes occurring on MS surface in the electrolyte and alteration of the corrosive electrolyte. Taking into consideration, the similar plot configuration of MS corrosion rate in the presence of GPP extract, it can be deduced, that increase in GPP concentration, despite significantly reducing the corrosion rate of MS has minimal influence on the corrosion behavior of MS. In the presence of the extracts, corrosion rate of MS initiated at values between 26.87 mm/y and 33.51 mm/y. The plot shows the corrosion rate decreased progressively with time signifying time dependent suppression effect of the extract molecules whereby the anions of the corrosion species are inhibited from getting to MS surface. Relative stability

was attained at 144 h where corrosion rate of MS varies between 5.44 mm/y and 10.06 mm/y. At 240 h, corrosion rate has marginally decreased to values between 3.451 mm/y and 8.937 mm/y. The image for MS corrosion in the presence of GPP extract (Fig. 2) shows the presence of GPP extract film which stifled the corrosion rate reactions on the steel surface. Observation of the inhibition efficiency values in Table 2 shows the final values at 240 h. The values varied from 95.16% at 1% GPP concentration to 98.13% at 2% GPP concentration confirming that GPP protection performance is independent of its concentration. Variation of inhibition efficiency with respect to time shows in Fig. 5(b) shows at 24 h inhibition efficiency varied between 57.14% and 65.64% before progressing to final values shown in Table 3.

ATF-FTIR Spectroscopy Studies

To further prove the adsorption of GPP on MS surface leading to the suppression of corrosion in the studied corrosive medium, the FTIR spectra of the crude GPP and the film extracted from the MS surface after corrosion were compared as shown in Fig. 7. In the GPP spectrum, the prominent absorption bands are at 3450 cm^{-1} , 2390 cm^{-1} , 1610 cm^{-1} , 1250 cm^{-1} , 1020 cm^{-1} , and 770 cm^{-1} . The broad band at 3450 cm^{-1} is assigned to O-H stretch and the band at 1610 cm^{-1} is due to the conjugated C=C stretching [49]. The absorption band at 1020 cm^{-1} is consistent with the C-O stretching of a primary alcohol [58] and the band at 770 cm^{-1} is associated with the alcohol, OH out-of-plane bending. This result, as expected show that the essential oils contained multiple organic compounds. Although the compositions and constituents of essential oils may vary depending on the geochemistry of the soil where it is cultivated, it is generally made up of terpenes such as terpineol, cineole, citronellal, and others [9]. Compared to the GPP, the spectrum of the extracted film exhibits all the absorption bands noted in the GPP spectrum. This provides experimental evidence to the claim of GPP molecules adsorption on the steel surface, which in extension is responsible for the inhibition of the metal against corrosion. Furthermore, it is observed that the C=C, C-O stretching, and the OH out-of-plane bending bands are sharper and more prominent in the extracted film spectrum relative to the raw GPP spectrum. This is suggestive of the involvement of these functional groups in the bonding process [29].

Fig 7

Download: [Download high-res image \(200KB\)](#)

Download: [Download full-size image](#)

Fig. 7. The FTIR spectra of the raw GPP (mixture of Ginger and Grape fruit oils) and the film extracted from the high carbon steel surface after immersion in 0.5M H₂SO₄ solution containing 3.5% GPP at room temperature.

Conclusion

Admixture of ginger and grapefruit essential oil effectively inhibited mild steel corrosion in dilute H₂SO₄ solution. ATF-FTIR data showed the oils contains multiple organic compounds and the corresponding spectrum of the extracted film GPP molecules adsorbed on the steel surface proves it is responsible for the inhibition of the metal against corrosion. Open circuit potential plots of the inhibited steel were significantly more electropositive relative to the plot without the oil extract. Passivation of the steel in the presence of the extract significantly altered the dynamics of the corrosion reaction processes.

Results from Potentiodynamic polarization and weight loss analysis confirmed the effective inhibition properties of the oil extract with inhibition efficiency generally above 90%.

Declaration of Competing Interest

No conflict of interest exists.

Acknowledgment

The author appreciates the support of Covenant University towards the successful actualization of this research.

References

[1]

Z. Ahmad

Selection of materials for corrosive environment

Principles of Corrosion Engineering and Corrosion Control, Elsevier Ltd (2006), 10.1016/B978-0-7506-5924-6.X5000-4

Google Scholar

[2]

M.T. Alhaffar, S.A. Umoren, I.B. Obot, A.A. IB Shaikh, M.M Solomon

Studies of the anticorrosion property of a newly synthesized Green isoxazolidine for API 5L X60 steel in acid environment

J. Mater. Res. Technol., 8 (2019), pp. 4399-4416

View PDF

View articleView in ScopusGoogle Scholar

[3]

H. Ashassi-Sorkhabi, M.R. Majidi, K. Seyyedi

Investigation of inhibition effect of some amino acids against steel corrosion in HCl solution

Appl. Surf. Sci., 225 (2004), pp. 176-185

View PDF

View articleView in ScopusGoogle Scholar

[4]

H. Ashassi-Sorkhabi, B. Masoumi, P.E. Ejbari

Corrosion inhibition of mild steel in acidic media by basic yellow 13 dye

J. Appl. Electrochem., 39 (9) (2009), pp. 1497-1501

[CrossrefView in ScopusGoogle Scholar](#)

[5]

Bahlakeh, M. Ramezanzadeh, B Ramezanzadeh

Experimental and theoretical studies of the synergistic inhibition effects between the plant leaves extract (PLE) and zinc salt (ZS) in corrosion control of carbon steel in chloride solution

J. Mol. Liq., 248 (2017), pp. 854-870

[View PDF](#)

[View articleView in ScopusGoogle Scholar](#)

[6]

A. Batah, M. Belkhaouda, L. Bammou, A. Anejjar, R. Salghi, A. Chetouani, L. Bazzi, B. B. Hammouti

Corrosion inhibition of carbon steel in acidic medium by Grapefruit oil extract

Mor. J. Chem., 5 (4) (2017), 10.48317/IMIST.PRSM/morjchem-v5i4.9797

[Google Scholar](#)

[7]

A. Berradja

Electrochemical techniques for corrosion and tribocorrosion monitoring: fundamentals of electrolytic corrosion

Singh A (Ed.), Corrosion Inhibitors, IntechOpen, London (2019), 10.5772/intechopen.85392

[Google Scholar](#)

[8]

K. Boumhara, M. Tabyaoui, C. Jama, F Bentiss

Artemisia Mesatlantica essential oil as green inhibitor for carbon steel corrosion in 1 M HCl solution: Electrochemical and XPS investigations

J. Ind. Eng. Chem., 29 (2015), pp. 146-155

[View PDF](#)

[View articleView in ScopusGoogle Scholar](#)

[9]

H. Boughendjioua, N.E.H. Mezedjeri, I. Idjouadiene

Chemical constituents of Algerian mandarin (*Citrus reticulata*) essential oil by GC-MS and FT-IR analysis

Curr. Issues Pharm. Med. Sci., 33 (2020), pp. 197-201

[CrossrefView in ScopusGoogle Scholar](#)

[10]

M. Bouoidina, A. Chaouch, A. Abdellaoui, B. Lahkimi, F. Hammouti, M. El-Hajjaji, A. Taleb, A. Nahle
Essential oil of "Foeniculum vulgare": antioxidant and corrosion inhibitor on mild steel immersed in hydrochloric medium

Anti-Corros. Method M., 64 (5) (2017), pp. 563-572

[View in ScopusGoogle Scholar](#)

[11]

W.D. Collins, R.E. Weyers, I.L. Al-Qadi

Chemical treatment of corroding steel reinforcement after removal of chloride-contaminated concrete

NACE Corros., 49 (1) (1993), pp. 74-88

[CrossrefView in ScopusGoogle Scholar](#)

[12]

G.C. Dariva, A.F. Alexandre

Corrosion inhibitors—principles, mechanisms and applications, developments in corrosion protection

Intechopen (2014), pp. 365-379, 10.5772/57255

[Google Scholar](#)

[13]

A. Dehghani, G. Bahlakeh, B. Ramezanzadeh, M. Ramezanzadeh

Electronic/atomic level fundamental theoretical evaluations combined with electrochemical/surface examinations of Tamarindus indica aqueous extract as a new green inhibitor for mild steel in acidic solution (HCl 1 M)

J. Taiwan Inst. Chem. E., 102 (2019), pp. 349-377

[View PDF](#)

[View articleView in ScopusGoogle Scholar](#)

[14]

A. Dehghani, F. Poshtiban, G. Bahlakeh, B. Ramezanzadeh

Fabrication of metal-organic based complex film based on three-valent samarium ions-[bis (phosphonomethyl) amino] methylphosphonic acid (ATMP) for effective corrosion inhibition of mild steel in simulated seawater

Constr. Build. Mater., 239 (117812) (2020)

[Google Scholar](#)

[15]

G. Dehghani, G. Bahlakeh, Ramezanzadeh

Green Eucalyptus leaf extract: A potent source of bio-active corrosion inhibitors for mild steel

Bioelectrochemistry, 130 (107339) (2019)

[Google Scholar](#)

[16]

D. Dwivedi, K. Lepkov, T. Becker

Carbon steel corrosion: A review of key surface properties and characterization methods

RSC Adv., 7 (2017), pp. 4580-4610

[View in Scopus](#)[Google Scholar](#)

[17]

U.J. Ekpe, U.J. Ibok, B.I. Ita, O.E. Offiong, E.E. Ebenso

Inhibitory action of methyl and phenylthiosemicarbazone derivatives on the corrosion of mild steel in hydrochloric acid

Mater. Chem. Phys., 40 (1995), pp. 87-93

[View PDF](#)

[View article](#)[View in Scopus](#)[Google Scholar](#)

[18]

Y. El Ouadi, A. Bouyanzer, L. Majidi, J. Paolini, J.M. Desjobert, J. Costa, A. Chetouani, B. Hammouti

Salvia officinalis essential oil and the extract as green corrosion inhibitor of mild steel in hydrochloric acid

J. Chem. Pharm. Res., 6 (7) (2014), pp. 1401-1416

[View in Scopus](#)[Google Scholar](#)

[19]

E. El Ouariachi, A. Bouyanzer, R. Salghi, B. Hammouti, J.M. Desjobert, J. Costa, J. Paolini, L. Majidi

Inhibition of corrosion of mild steel in 1 M HCl by the essential oil or solvent extracts of *Ptychotis verticillata*

Res. Chem. Intermed., 41 (2015), pp. 935-946

[CrossrefView in ScopusGoogle Scholar](#)

[20]

B.R. Fazal, T. Becker, B. Kinsella, K. Lepkova

A review of plant extracts as green corrosion inhibitors for CO₂ corrosion of carbon steel

npj Mater. Degrad., 6 (5) (2022)

[Google Scholar](#)

[21]

P. Feng, K. Wan, G. Cai, L. Yang, Y Li

Synergistic protective effect of carboxymethyl chitosan and cathodic protection of X70 pipeline steel in seawater

RSC Adv., 7 (2017), pp. 3419-3427

[View in ScopusGoogle Scholar](#)

[22]

A. Fidrusli, Suryanto, M Mahmood

Ginger extract as green corrosion inhibitor of mild steel in hydrochloric acid solution

IOP Conf. Ser.: Mater. Sci. Eng., 290 (2018), Article 012087, 10.1088/1757-899X/290/1/012087

[View in ScopusGoogle Scholar](#)

[23]

A.S. Fouda, A.A. Nazeer, M. Ibrahim, M. Fakh

Ginger extract as green corrosion inhibitor for steel in sulfide polluted salt water

J. Kor. Chem. Soc., 57 (2) (2013), pp. 272-278, 10.5012/jkcs.2013.57.2.272

[Google Scholar](#)

[24]

S. Fu, L. Li, Y. Cao, L. Wang, L. Yan, L. Lu

Tryptophan as green corrosion inhibitor for low carbon steel in hydrochloric acid solution

J. Mater. Sci., 45 (2010), pp. 979-986

[CrossrefView in ScopusGoogle Scholar](#)

[25]

H.S. Gadow, M.M. Motawea

Investigation of the corrosion inhibition of carbon steel in hydrochloric acid solution by using ginger roots extract

RCS Adv., 40 (7) (2017), pp. 24576-24588

[View in ScopusGoogle Scholar](#)

[26]

F. García-Labiano, L.F. de Diego, A. Cabello, P. Gayán, A. Abad, J. Adánez, G. Sprachmann

Sulphuric acid production via Chemical Looping Combustion of elemental Sulphur

Appl. Energy, 178 (2016), pp. 736-745, 10.1016/j.apenergy.2016.06.110

[View PDF](#)

[View articleView in ScopusGoogle Scholar](#)

[27]

H. Gerengi, N. Sen, I. Uygur, M.M. Solomon

Corrosion response of ultra-high strength steels used for automotive applications

Mater. Res. Express., 6 (0865a6) (2019), 10.1088/2053-1591/ab2178

[Google Scholar](#)

[28]

Z. Ghazi, H. Elmsellem, M. Ramdani, A. Chetouani, R. Rmil, A. Aouniti, C. Jama, B. Hammouti

Corrosion inhibition by naturally occurring substance containing Opuntia-Ficus Indica extract on the corrosion of steel in hydrochloric acid

J. Chem. Pharm. Res., 6 (2014), pp. 1417-1425

[View in ScopusGoogle Scholar](#)

[29]

S.A. Haladu, S.A. Umoren, S.A. Ali, M.M. Solomon, A-R.I. Mohamed

Synthesis, characterization and electrochemical evaluation of anticorrosion property of a tetrapolymer for carbon steel in strong acid media

Chin. J. Chem. Eng. (2019), pp. 965-978

[View PDF](#)

[View article](#)[View in Scopus](#)[Google Scholar](#)

[30]

E. Hamdani, O. El Ouariachi, A. Mokhtari, N. Salhi, B. Chahboun, A. ElMahi, A. Bouyanzer, B. Zarrouk, J. Hammouti, Costa

Chemical constituents and corrosion inhibition of mild steel by the essential oil of *Thymus algeriensis* in 1.0 M hydrochloric acid solution

Der. Pharm. Chem., 7 (8) (2015), pp. 252-264

[View in Scopus](#)[Google Scholar](#)

[31]

S.M.Z. Hossain, S.A. Razzak, M.M. Hossain

Application of essential oils as green corrosion inhibitors

Arab. J. Sci. Eng., 45 (2020), pp. 7137-7159

[Crossref](#)[View in Scopus](#)[Google Scholar](#)

[32]

C.H. Hsu, F. Mansfeld

Concerning the conversion of the constant phase element parameter Y_0 into a capacitance

Corrosion, 57 (9) (2001), pp. 747-748

[Crossref](#)[View in Scopus](#)[Google Scholar](#)

[33]

Y. Jiang, Y. Liu, S. Gao, X. Guo, J. Zhang

Experimental and theoretical studies on corrosion inhibition behavior of three imidazolium-based ionic liquids for magnesium alloys in sodium chloride solution

J. Mol. Liq. (116998) (2022), p. 345

[Google Scholar](#)

[34]

F.S. Kadhim

Investigation of carbon steel corrosion in water base drilling mud

Mod. Appl. Sci., 5 (1) (2011)

[Google Scholar](#)

[35]

L. Khaksar, J. Shirokoff

Effect of elemental sulfur and sulfide on the corrosion behavior of Cr-Mo low alloy steel for tubing and tubular components in oil and gas industry

Materials, 10 (2017), p. 430

[CrossrefView in ScopusGoogle Scholar](#)

[36]

Y.I. Kuznetsov

Organic inhibitors of corrosion of metals

Springer US (1996), 10.1007/978-1-4899-1956-4

[Google Scholar](#)

[37]

A. Lahhit, J.M. Bouyanzer, B. Desjobert, R. Hammouti, J. Salghi, C. Costa, F. Jama, Bentiss, L Majidi

Fennel (Foeniculum Vulgare) essential oil as green corrosion inhibitor of carbon steel in hydrochloric acid solution

Port. Electrochim. Acta., 29 (2) (2011), pp. 127-138

[CrossrefView in ScopusGoogle Scholar](#)

[38]

Y. Li, P. Zhao, Q. Liang, B. Hou

Berberine as a natural source inhibitor for mild steel in 1 M H₂SO₄

Appl. Surf. Sci., 252 (2005), pp. 1245-1253

[View PDF](#)

[View articleView in ScopusGoogle Scholar](#)

[39]

G.Q. Liu, Z.Y. Zhu, W. Ke, C.I. Han, C.L. Zeng

Corrosion behavior of stainless steels and nickel-based alloys in acetic acid solutions containing bromide ions

NACE Corros., 57 (8) (2001), pp. 730-738

[CrossrefView in ScopusGoogle Scholar](#)

[40]

R.T. Loto, C.A. Loto

Effect of P-phenyldiamine on the corrosion of austenitic stainless steel type 304 in hydrochloric acid

Int. J. Elect. Sci., 7 (10) (2012), pp. 9423-9440

[View PDF](#)

[View articleView in ScopusGoogle Scholar](#)

[41]

R.T. Loto

Comparative study of the pitting corrosion resistance, passivation behavior and metastable pitting activity of NO7718, NO7208 and 439L super alloys in chloride/sulphate media

J. Mater. Res. Techn., 8 (1) (2019), pp. 623-629

[View PDF](#)

[View articleView in ScopusGoogle Scholar](#)

[42]

R.T. Loto

Corrosion inhibition studies of the combined admixture of 1,3-diphenyl-2-thiourea and 4-hydroxy-3-methoxybenzaldehyde on mild steel in dilute acid media

Rev. Colomb. Quim., 46 (1) (2017), pp. 20-32

[CrossrefView in ScopusGoogle Scholar](#)

[43]

R.T. Loto

Study of the synergistic effect of 2-methoxy-4-formylphenol and sodium molybdenum oxide on the corrosion inhibition of 3CR12 ferritic steel in dilute sulphuric acid

Result. Phys., 7 (2017), pp. 769-776

[View PDF](#)

[View articleView in ScopusGoogle Scholar](#)

[44]

C.A. Loto, R.T. Loto, O.O. Joseph, A.P.I. Popoola

Corrosion inhibitive behaviour of camellia sinensis on aluminium alloy in H₂SO₄

Int. J. Elect. Sci., 9 (3) (2014), pp. 1221-1231

[View PDF](#)

[View articleView in ScopusGoogle Scholar](#)

[45]

R.T. Loto, R. Leramo, B. Oyebade

Synergistic combination effect of *salvia officinalis* and *lavandula officinalis* on the corrosion inhibition of low-carbon steel in the presence of SO₄²⁻ and Cl⁻ containing aqueous environment

J. Fail. Anal. & Preven., 18 (6) (2018), pp. 1429-1438

[CrossrefView in ScopusGoogle Scholar](#)

[46]

N. Mohanan, Palaniswamy

Corrosion inhibition of mild steel by ethanolic extracts of *Ricinus communis* leaves

Indian J. Chem. Technol., 12 (2005), pp. 356-360

[Google Scholar](#)

[47]

Monticelli

Corrosion Inhibitors

Wandelt Klaus (Ed.), Encyclopedia of Interfacial Chemistry, Elsevier, Amsterdam (2018), pp. 164-171, 10.1016/B978-0-12-409547-2.13443-2

[View PDF](#)

[View articleView in ScopusGoogle Scholar](#)

[48]

H. Müller

Sulfuric Acid and Sulfur Trioxide" in Ullmann's Encyclopedia of Industrial Chemistry

Wiley-VCH, Weinheim (2000), p. 2000, 10.1002/14356007.a25_635

[Google Scholar](#)

[49]

A.B.D. Nandiyanto, R. Oktiani, R. Ragadhita

How to read and interpret FTIR spectroscopy of organic material

Indones. J. Sci. Technol., 4 (2019), pp. 97-118

[CrossrefView in ScopusGoogle Scholar](#)

[50]

J. Narenkumar, P. Parthipan, A.U.R. Nanthini, G. Benelli, K. Murugan, A. Rajasekar

Ginger extract as green biocide to control microbial corrosion of mild steel

3 Biotech., 7 (2) (2017), p. 133, 10.1007/s13205-017-0783-9

[View in Scopus](#)[Google Scholar](#)

[51]

ÖZcan

AC impedance measurements of cysteine adsorption at mild steel/sulphuric acid interface as corrosion inhibitor

J. Solid State Electrochem., 12 (2008), pp. 1653-1661

[Crossref](#)[View in Scopus](#)[Google Scholar](#)

[52]

M. Palomar-Pardavé, M. Romero-Romo, H. Herrera-Hernández, M.A. Abreu-Quijano, N.V. Likhanova, J. Uruchurtu, J.M. Juárez-García

Influence of the alkyl chain length of 2 amino 5 alkyl 1, 3, 4 thiadiazole compounds on the corrosion inhibition of steel immersed in sulfuric acid solutions

Corros. Sci., 54 (2012), pp. 231-243

[View PDF](#)

[View article](#)[View in Scopus](#)[Google Scholar](#)

[53]

J.C. Philip

Survey of Industrial Chemistry

John Wiley & Sons, New York (1987), pp. 45-57

[Google Scholar](#)

[54]

F. Presuel-Moreno, M.A. Jakab, N. Tailleart, M. Goldman, J.R. Scully

Corrosion-resistant metallic coatings

Mater. Today., 11 (10) (2008), pp. 14-23

[View PDF](#)

[View article](#)[View in Scopus](#)[Google Scholar](#)

[55]

G. Quartarone, L. Ronchin, A. Vavasori, C. Tortato, L. Bonaldo

Inhibitive action of gramine towards corrosion of mild steel in deaerated 1.0 M hydrochloric acid solutions

Corros. Sci., 64 (2012), pp. 82-89

[View PDF](#)

[View article](#)[View in Scopus](#)[Google Scholar](#)

[56]

M. Ramezanzadeh, Z. Sanaei, G. Bahlakeh, B. Ramezanzadeh

Highly effective inhibition of mild steel corrosion in 3.5% NaCl solution by green Nettle leaves extract and synergistic effect of eco-friendly cerium nitrate additive: Experimental, MD simulation and QM investigations

J. Mol. Liq., 256 (2018), pp. 67-83

[View PDF](#)

[View article](#)[View in Scopus](#)[Google Scholar](#)

[57]

L.M. Rivera-Grau, M. Casales, I. Regla, D.M. Ortega-Toledo, J.A. Ascencio-Gutierrez, J. Porcayo-Calderon, L. Martinez-Gomez

Effect of organic corrosion inhibitors on the corrosion performance of 1018 carbon steel in 3% NaCl solution

Int. J. Elect. Sci., 8 (2013), pp. 2491-2503

[View PDF](#)

[View article](#)[View in Scopus](#)[Google Scholar](#)

[58]

T.S.T. Saharuddin, L.N. Ozair, A.S. Zulkifli, N.S.H. Shah, N.S. Sahidan

Characterization of encapsulated ginger essential oils and its antimicrobial properties

J. Acad. (2020), pp. 1-6

[Crossref](#)[Google Scholar](#)

[59]

M.S. Sanusi, S.R. Shamsudin, A. Rahmat, R. Wardan

Electrochemical corrosion behaviours of AISI 304 austenitic stainless steel in NaCl solutions at different pH

AIP Conf. Proc., 2030 (020116) (2018)

[Google Scholar](#)

[60]

Saratha, N. Kasthuri, P. Thilagavathy

Environment friendly acid corrosion inhibition of mild steel by Ricinus communis leaves

Der. Pharma. Chem., 1 (2) (2009), pp. 249-257

[Google Scholar](#)

[61]

R.A.L. Sathiyathan, M.M. Essa, S. Maruthamuthu, M. Selvanayagam, N. Palaniswamy

Inhibitory effect of Ricinus communis (Castor-oil plant) leaf extract on corrosion of mild steel in low chloride medium

J. Indian Chem. Soc., 82 (4) (2005), pp. 357-359

[View in Scopus](#)[Google Scholar](#)

[62]

J.Y. Sha, H.H. Ge, C. Wan, L-T. Wang, S-Y. Xie, X-J. Meng, Y-Z. Zhao

Corrosion inhibition behaviour of sodium dodecyl benzene sulphonate for brass in an Al₂O₃ nanofluid and simulated cooling water

Corros. Sci., 148 (2019), pp. 123-133

[View PDF](#)

[View article](#)[View in Scopus](#)[Google Scholar](#)

[63]

D.D.N. Singh, T.B. Singh, B. Gaur

The role of metal cations in improving the inhibitive performance of hexamine on the corrosion of steel in hydrochloric acid solution

Corros. Sci., 37 (6) (1995), pp. 1005-1019

[View PDF](#)

[View article](#)[View in Scopus](#)[Google Scholar](#)

[64]

H. Venzlaff, D. Enning, J. Srinivasan, K.J.J. Mayrhofer, A.W. Hassel, F. Widdel, M. Stratmann

Accelerated cathodic reaction in microbial corrosion of iron due to direct electron uptake by sulfate-reducing bacteria

Corros. Sci., 66 (2013), pp. 88-96

[View PDF](#)

[View articleView in ScopusGoogle Scholar](#)

[65]

C. Wang, C. Zou, Y. Cao

Electrochemical and isothermal adsorption studies on corrosion inhibition performance of β -cyclodextrin grafted polyacrylamide for X80 steel in oil and gas production

J. Mol. Struct., 1228 (129737) (2021)

[Google Scholar](#)

[66]

D.A. Winkler

Predicting the performance of organic corrosion inhibitors

Metals, 7 (12) (2017), p. 553, 10.3390/met7120553

[View in ScopusGoogle Scholar](#)

[67]

N. Yilmaz, A. Fitoz, U. Ergun, K.C. Emregul

A combined electrochemical and theoretical study into the effect of 2-((thiazole-2-ylimino)methyl)phenol as a corrosion inhibitor for mild steel in a highly acidic environment

Corros. Sci., 111 (2016), pp. 110-120

[View PDF](#)

[View articleView in ScopusGoogle Scholar](#)

[68]

M. Znini

Application of essential oils as green corrosion inhibitors for metals and alloys in different aggressive mediums - a review

Arab. J. Med. Aromat. Plant., 3 (5) (2019)

[Google Scholar](#)

[69]

M. Bathily, B. Ngom, D. Gassama, S. Tamba

Review on essential oils and their corrosion-inhibiting properties

Am. J. Appl. Chem., 9 (3) (2021), pp. 65-73

[Crossref](#) [Google Scholar](#)

Cited by (9)

Unlocking the power of Inula Viscosa essential oil: A green solution for corrosion inhibition in XC48 steel within acidic environments

2024, Process Safety and Environmental Protection

Citation Excerpt :

Recently, the focus of various studies has been the employing of essential oils as green metal corrosion inhibitors. In particular, investigations was made into essential oils from sources like ginger and grapefruit (Loto and Solomon, 2023), cinnamon (Dahmani et al., 2021; Lazrak et al., 2021), nutmeg (Abdallah et al., 2020), Asteriscus graveolens and Pulicaria incisa (Chaib et al., 2020), Thymbra capitata (L.) (Moukhles et al., 2020), Cupressus Arizonica (Cherrad et al., 2020), Ammi visnaga (L.) (Chraka et al., 2020), Ammodaucus leucotrichus (Manssouri et al., 2021), Ocimum basilicum (Ansari et al., 2021), Elettaria cardamomum (Tarfaoui et al., 2021), and Foeniculum vulgare bulb (Bouoidina et al., 2017). Natural materials, according to these investigations, often contain organic substances such as tannins, flavonoids, alkaloids, and nitrogenous bases.

[Show abstract](#)

Principles and theories of green chemistry for corrosion science and engineering: design and application

2024, Green Chemistry

2023, Polymers

[View all citing articles on Scopus](#)

© 2022 The Author(s). Published by Elsevier B.V. on behalf of African Institute of Mathematical Sciences / Next Einstein Initiative.

[Recommended articles](#)

Experimental and theoretical studies on protecting steel against 0.5 M H₂SO₄ corrosion by new schiff base

Journal of the Indian Chemical Society, Volume 99, Issue 9, 2022, Article 100665

Hojat Jafari, ..., Avni Berisha

Evaluation of the green inhibitor effect on the corrosion of pipeline steel in NS4 medium

Procedia Structural Integrity, Volume 36, 2022, pp. 313-317

Tetyana Kalyn, ..., Liubov Poberezhna

[View PDF](#)

Corrosion inhibition effect of citrus sinensis essential oil extract on plain carbon steel in dilute acid media

South African Journal of Chemical Engineering, Volume 35, 2021, pp. 159-164

Roland Tolulope Loto, ..., Jennifer Iruoma Ugada

[View PDF](#)